MECHANICAL BEHAVIOUR OF JUTE FIBRE-REINFORCED POLYESTER COMPOSITE: CHARACTERIZATION OF DAMAGE MECHANISMS USING ACOUSTIC EMISSION.

A. Alia[1,2*], G. Fantozzi[1], N. Godin[1], H. Osmani[2], P. Reynaud[1]

[1]INSA of Lyon, MATEIS, University of Lyon, 7 avenue Jean Capelle, 69621, Villeurbanne, France
[2]IOMP, LMNM, University of Setif, *Campus (Ex-travaux publics), Avenue Saïd Boukhraïssa, 19000 Sétif* Algeria
*Adem.alia@insa-lyon.fr

Keywords: natural fibre, tensile, fatigue, acoustic emission, composite damage.

Abstract
In this paper, a mechanical characterization of a woven jute fabric reinforced polyester composite is conducted under both monotonic and cyclic fatigue tensile loading. Two stacking sequences were considered: $[0]_8$ and $[+45/-45]_{2S}$. Tensile static tests were performed at a constant rate of 0.1mm/min and fatigue tests were performed in tension/tension mode with a stress ratio of R=0.01 and a frequency of 1 Hz. The acoustic emission (AE) technique as well as microstructural analyzes were used to characterize the different damage modes and to follow their evolution during tests.

1. Introduction

Nowadays, mechanical behaviour of natural plant fibre reinforced polymers (NFRP) is widely studied and the applications of these composites as structural materials exhibit a growing interest. The natural plant fibres used as reinforcement of composites are ligno-cellulosic fibres such as flax, hemp, jute, kenaf, etc. These fibres exhibit good specific mechanical properties, low density and low cost compared to the carbon and glass fibres. The large majority of papers concerning this type of composites is related to flax fibre reinforced polymers, very few of them deals with the mechanical behaviour of jute fibre reinforced polymers. In order to improve the mechanical properties of the NFRP, it is important to characterize the different damage modes responsible for the mechanical behaviour of the composites. The acoustic emission (AE) technique [1,2] and microstructural analysis (using scanning electron microscopy (SEM)) are good tools to identify the damage mechanisms and to follow their evolution during tests. To further promote the use of this natural fibre reinforced composite, it is very important to characterize it in fatigue behaviour, which is not widely studied in the literature and most of works concerning the fatigue behaviour of these composites are relatively recent. For example, de Vasconcellos et al. [3] studied the cyclic fatigue behaviour of woven hemp/epoxy composite in tension-tension mode and Liang et al. [4] studied the fatigue behaviour of flax reinforced composite. Concerning works on jute fibre reinforced composite, Dobah et al. [5] have studied the multiaxial mechanical behaviour of jute/polyester composite in both static and fatigue tests.

Thus, in this paper, a characterization of a woven jute/polyester composite is proposed under both monotonic and cyclic fatigue tensile loading. Damage mechanisms are analyzed using AE technique and microstructural analyses.

2. Materials and methods

2.1. Fabrication of laminates

In this work, the studied composites are made of 8 plies of balanced taffetas jute fabrics impregnated with polyester resin. The jute fabric is produced by Complexe de jute company (Bejaia, Algeria) and the polyester resin is the PD-6191 supplied by Maghreb Pipe factory (M'sila, Algeria). The composite plates are manufactured at the LMNM laboratory (Setif, Algeria) using a hand lay-up composites fabrication technique at room temperature. They are characterized by a fibre volume fraction of 28 ± 2% and a maximum void content of around 2 %. The void content was measured by tomography observation. Two stacking sequences were considered in this work: the first one, referred as $[0]_8$ (noted [0]) , has the weft direction of each ply oriented at 0° from the tensile axis, the second one , referred as $[+45/-45]_{2S}$ (noted [±45]) has the weft direction of each ply oriented alternatively at +45° and -45° from the tensile axis. Finally, specimens were cut (without lubrication) from the obtained laminate plates with dimensions of 160mm×15mm×8mm and with a gripping length of 30 mm of each edge.

2.2. Testing method

The mechanical tests were carried out at MATEIS laboratory using a MTS 810 hydraulic testing system equipped with a 100 kN capacity load cell. All tests were conducted at room temperature. Tensile static tests were performed at a constant rate of 0.1 mm/min and fatigue tests were performed in tension/tension mode with a stress ratio of R=0.01 and a frequency of 1 Hz under load control. In order to establish the stress lifetime diagram of the composite, at least, four specimens were tested to failure at a minimum of four levels of stress (50%, 60%, 70% and 80% of ultimate strength σ_f).

2.3. Acoustic emission

AE monitoring was performed continuously during the monotonic tensile and fatigue tests. A two-channel data acquisition system (PCI 2) supplied by Mistras Group Company was used for the measurements of the AE. The AE signals were recorded by two resonant Micro-80 piezoelectric sensors with a bandwidth of 100 kHz to 1MHz and a resonance peak of around 300 kHz. The sensors were placed on the surface of the specimens at the gauge length extremities and spacing of 70 mm. A pencil lead break procedure was used for the calibration of the data acquisition system and to define the different acquisition parameters : PDT (Peak Definition Time) =10 µs, HDT (Hit Definition Time) =20 µs and HLT (Hit Lockout Time) =1000 µs. The detection threshold was set at 40 dB in order to avoid noise acquisition. In addition, velocity of the AE waves was also measured for each kind of specimen and only events located between the sensors were used to analyse the AE data.

The AE data were processed using MATLAB Software. The aim of this analysis is intended to identify the acoustic signatures of the different damage mechanisms involved in the studied composite materials by using an unsupervised pattern recognition method and by considering both temporal and frequential features. 24 descriptors were considered and by means of the Laplacian score and dendrogram (correlation analysis), only three relevant and uncorrelated descriptors were retained for the clustering : one temporal descriptor (duration), and two frequential descriptors (centroid frequency and peak frequency). The clustering was then conducted on the selected features by combining a PCA analysis and *k-means* (optimized by a genetic algorithm). The optimal number of clusters *k* was determined by using the Davies & Bouldin criterion and the Silhouette index.

3. Results and discussion

3.1. Quasi-static behaviour

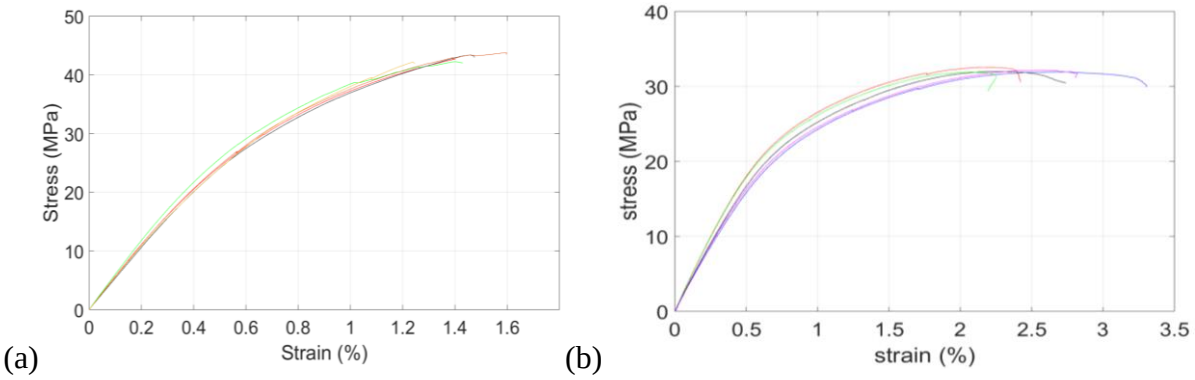

Figure 1. Tensile stress-strain behaviour of jute laminates. (a) [0], (b) [±45]

Fig. 1 shows the tensile stress-strain curves of five tested JFRP specimens for the two layups : [0] and [±45]. It can be observed that the curves are mainly composed of two parts. The first linear part, is associated with the elastic behaviour of the composite materials, followed by a non-linear one until the final failure of the specimens reflecting the initiation and the development of the damage within the samples. Notice that the second non linear part is more pronounced for the [±45] samples, meaning that the specimens exhibited more internal plastic deformation and damage prior to final failure.
For the [0] laminates, the measured tensile strength σ_f was 42.9 (±3.3) MPa for a maximum strain of about 1.38 %. The Young's modulus was calculated on the fist part of the curve and was found equal to 5.9 (±0.23) GPa. For the [±45] laminates tensile strength was σ_f =31.1 (±1.1) MPa for a maximum strain around 2.7 % and the Young's modulus was about 3.6 (±0.3) GPa. A good repeatability of tests on composites can be observed, particularly on the initial part of the curves. This, may be explained by the averaging effect on the composite scale. Indeed, under mechanical loading, the response of all the reinforcements creates a compensation effect of the disparities between fibres. This results in a smaller scale dispersion of the laminates.

Fig. 2 shows the SEM observations conducted on the broken samples for the two layups. The images reveal numerous fibre-matrix debondings (1), they are more marked for [±45] specimens than for [0] samples. Some transverse matrix cracks (2) are also observed on the micrographs. They seems to be initiated inside the jute yarn, then propagated into the matrix-rich zone. Moreover, the SEM observations of fractured surfaces show that the broken fibres are pulled out from the matrix and no matrix residue was observed on their surfaces (3). This indicates that the interface between fibres and matrix is relatively weak.

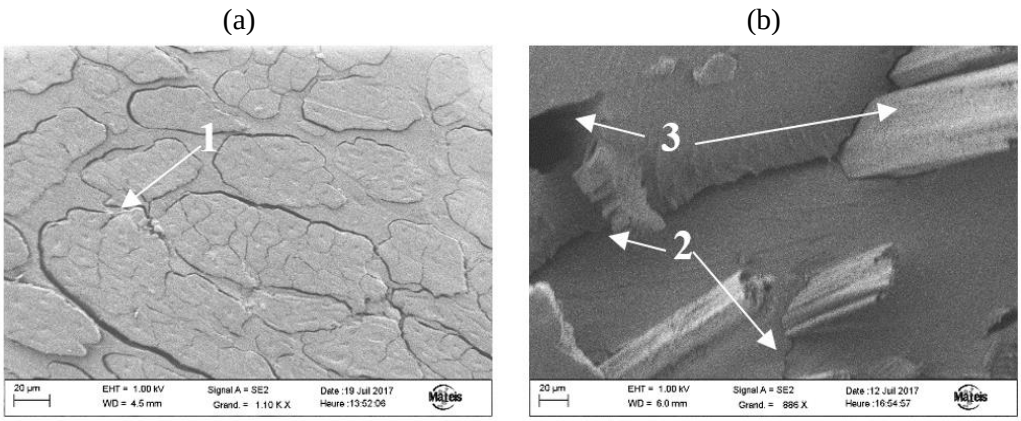

Figure 2. SEM obervations of the broken samples. (a) [±45], (b) [0]

3.2. Classification results

The application of the clustering methodology described in section 2.3 returned the following results. Three classes of signals were obtained for the two types of composites. Fig. 3 presents the separation of these clusters in amplitude-time diagram, superposed with the stress-strain curve for the two layups. It can be observed that the class 1 and class 2 present an important overlaping. So, amplitude seems to be unable to separate properly the three clusters. Thus, a comparison between the other parameters of the three clusters was conducted. The results are summarized in Table. 1

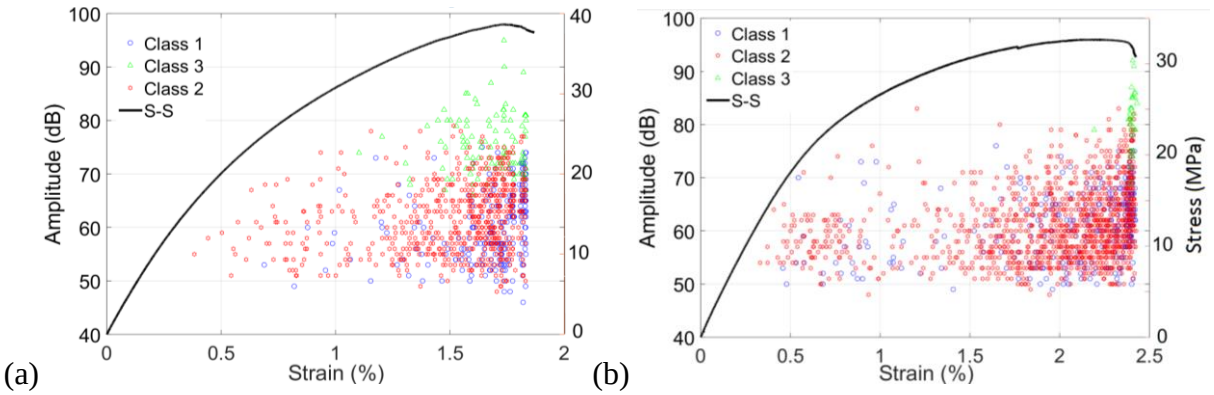

Figure 3. Ampltitude of events for the obtained classes superposed with the stress-strain curve. (a) [0], (b) [±45]

For the two layups, similar mean charateristics were observed for each class. It can be seen that class 1 and class 2 exhibit almost similar temporal characteristics. The frequential features are the parameters that differentiate the most these two classes. So, it is very important to consider both temporal and frequential descriptors for clustering in order to obtain a relevant segmentation. The third class which is quite different regarding to the temporal characteristics (the highest amplitude, and the longest duration) has a similar centroid frequency to that of the class 1 and a similar peak frequency to that of the class 2.

Table 1. characteritics of the three obtained classes

	Classe 1	Classe 2	Classe 3	Resin
Rise time (µs)	22	18	20	20
Counts	16	22	30	20
Durations (µs)	153	120	319	189
Amplitude (dB)	59	62	72	58
Abs E (attoJ)	600	1100	15000	216
Average frequency (kHz)	114	178	99	80
Decay frequency (kHz)	90	157	80	60
Rise frequency (kHz)	222	300	300	350
Centroid frequency (kHz)	246	300	250	300
Peak frequency (kHz)	34	322	307	30

Fig. 4 presents the cumulative number of events for each class with respect to time. It is an indication of the chronology of apparition of the three classes. For the two lay-ups, the class 2 which contains the biggest number of events, appears earlier during the tensile test, followed by the occurrence of the class 1. The third class, which contains the lowest number of events, appears around the half of the tensile test for the [0] specimens, whereas, for the [±45] specimen, it occurs few time before the final failure of the specimens.

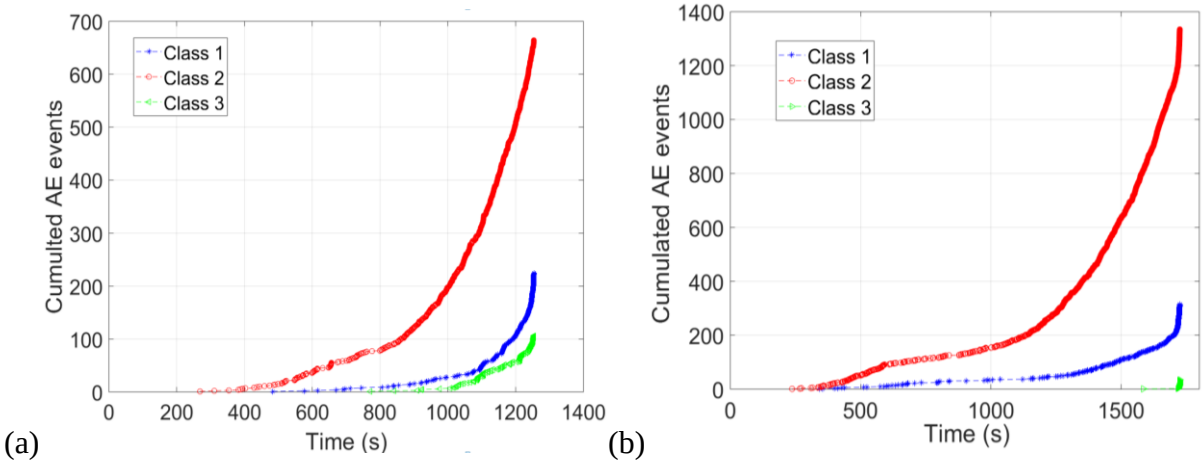

(a) (b)

Figure 4. Chronology of apparition of the three clusters as a function of time. (a) [0], (b) [±45]

In order to associate the obtained clusters to the corresponding damage mechanism, tests on pure polyester resin monitored with AE were firstly conducted. The obtained results showed that signals collected on pure resin had similar characteristics to that of the class 1 (Table. 1). Thus, signals of class 1 may be attributed to the matrix crackings.

Afterthat, interrupted tensile tests were performed on [0] samples. The first one was conducted up to 60% of σ_f which corresponds only to the appearance of class 2. The second one was performed up to 75% of σ_f which corresponds to an increase of the class 2 and the appearance of the class 1. SEM micrographic observations for test conducted up to 60% of σ_f showed essentially fibre-matrix debondings (Fig. 5a). No matrix cracks were observed. So the class 2 may be assigned to the fibre-matrix debondings. Moreover, the images of the sample tested up to 75% of σ_f showed that the debondings are more developed and the occurence of some matrix cracks (Fig. 5b) which support the assignment of the class 1 to the matrix crackings. Finally, the remaining class (class 3), contains the lowest number of signals which present the highest amplitude, highest energy and which occurs few time before the final failure of the specimen, may be attributed to fibre breakages.

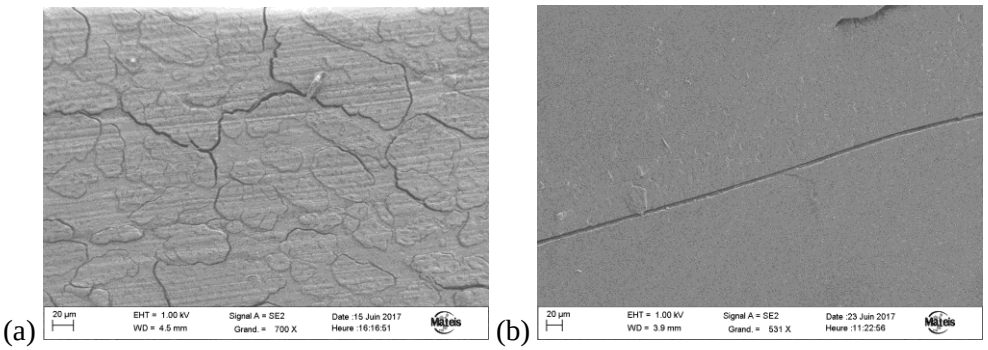

(a) (b)

Figure 5. SEM image of the [0]. (a) sample tested up 60% of σ_f, (b) sample tested up 75% of σ_f

3.3. Fatigue behaviour

3.3.1 S-N curve

Fatigue tests were performed for the [0] specimens. Four samples were tested per stress level. The average number of fatigue cycles until failure (*Nf*) with the standard deviation between brackets are given in Table 2.

Table 2. Average number of cycles to failure for the different stress levels (standard deviation between brackets).

	$0.5\ \sigma_f$	$0.6\ \sigma_f$	$0.7\ \sigma_f$	$0.8\ \sigma_f$
N_f	263527 (128856)	48863 (26732)	24294 (9570)	4292 (1530)

The S-N fatigue lifetime diagram of the studied composite is shown in Fig. 6. Points on diagram present the experimental values while the red line presents the S-N curve determined by Wöhler model (Eq. 1).

$$Log\ (Nf)=A-B\sigma_{max\text{-}fat} \quad (1)$$

where *Nf* is the number of cycles at failure, *A* and *B* are material parameters and $\sigma_{max\text{-}fat}$ is the maximum fatigue loading stress. In Fig. 6, it can be noticed that there is a significant scattering in fatigue lifetime of the composite. It may be due to the natural dispersion of the mechanical properties of the composite.

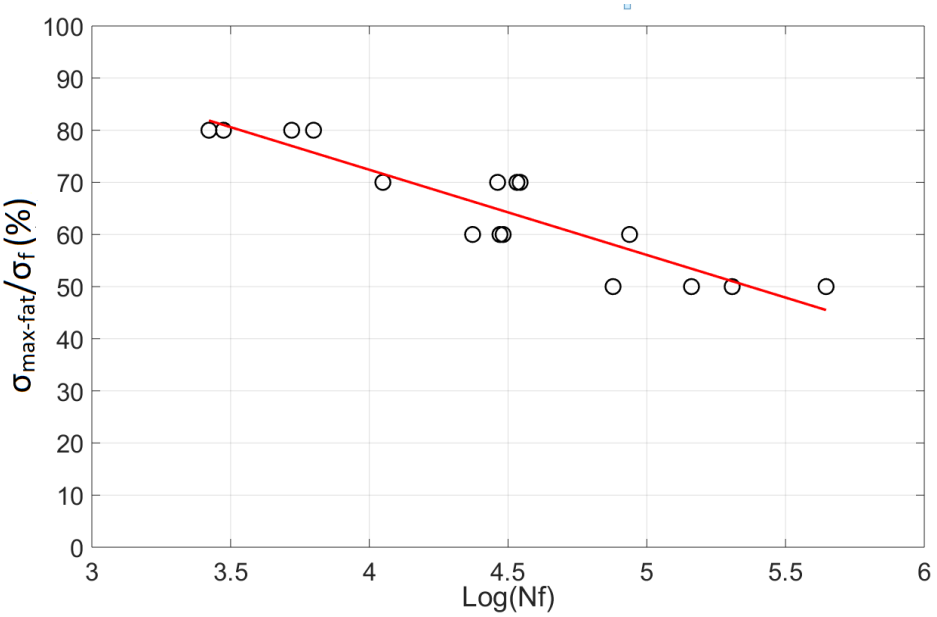

Figure 6. S-N curve for [0] jute/polyester composite.

3.3.2 Damage analysis

During fatigue tests, four mechanical parameters (illustrated in Fig. 7a) were determined for each cycle: the secant modulus (slope of the axis of the hysteresis loop) , hysteresis energy (corresponding to the area enclosed within the loop), the maximum and the residual strain for the considered cycle.

The evolution of these mechanical parameters during the fatigue tests is a good damage indicator. Fig. 7b-d illustrate the variation of these parameters as a function of the normalized number of cycles (N/Nf). Fig. 7b shows the evolution of the secant modulus normalized by the measured modulus during the first cycle for each stress level. It can be seen that for the high stress levels (80% and 70% of σ_f), the modulus decreases with a linear trend during the most part of the specimens lifetime reflecting the damage development. Towards the end of the tests a strong acceleration of the decrease is observed leading to the final failure of samples. For the tests conducted at 60% of σ_f the modulus is almost constant during the fatigue test with a significant decrease at the end of the tests. For samples loaded at 50% of σ_f, an increase of the modulus is firstly observed at the beginning of the fatigue test, then it decreases slightly with some fluctuations until the end of the test where it suddenly drops. The increase and the fluctuation of the modulus for low stress levels are maybe due to the stiffening effect of the composite samples caused by the reorientation of the microfibrils within jute fibres. It is more visible under the low stress levels, because the damage is less extended when compared to high stress levels.

Fig. 7c shows the evolution of the maximum and residual strains. It can be noticed that the two strains exhibit the same trend. Whatever the stress level, three distinct zones are observed: at the beginning, the strain starts with a strong increase; then, during the main part of the test, a steady increase with a linear trend is observed and finally the strain increases significantly just before the final failure of the specimens.

The evolution of the hysteresis energy is illustrated in Fig. 7d. It is noticed that the higher the stress level , the more important the dissipated energy, because of the increment of the loop size. As for the strain, three zones of evolution are observed on hysteresis energy evolution.

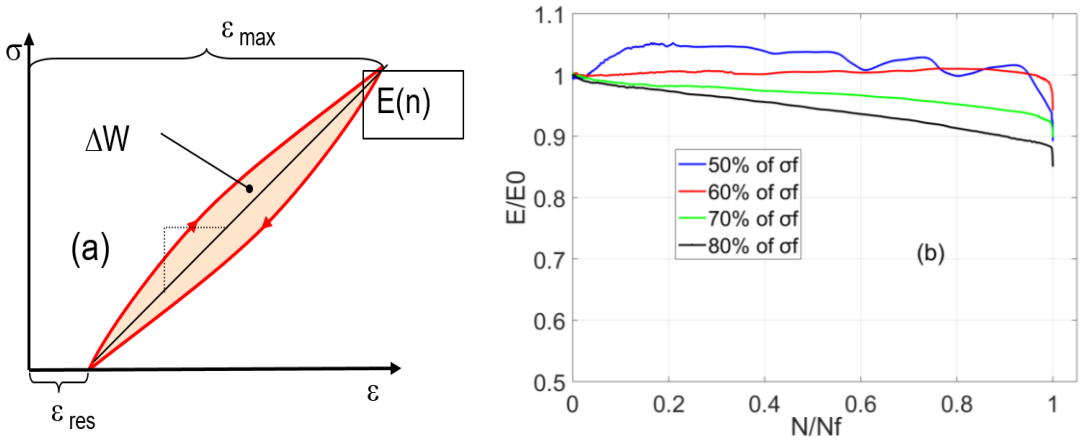

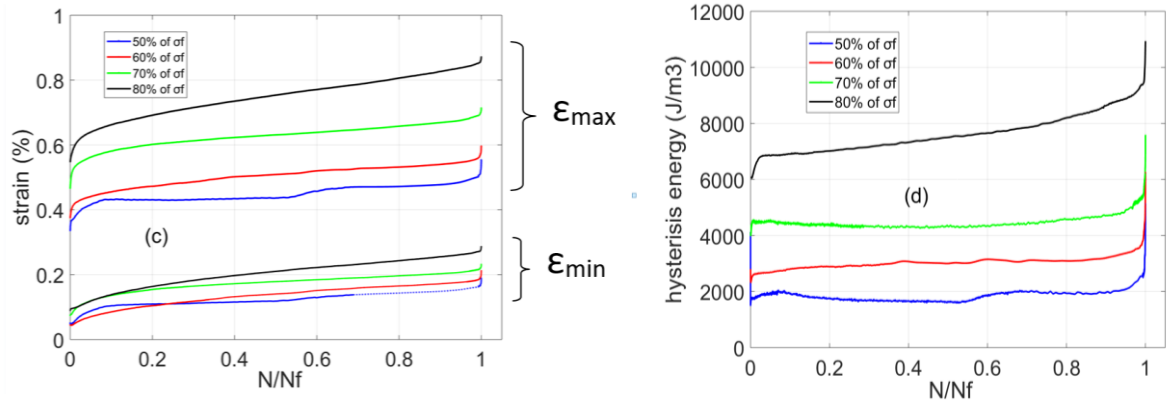

Figure 7. Mechanical parameters as a function of the normalized cycle number. (a) illustration of the different parameters, (b) Normalized elastic modulus, (c) maximum and residual strains, (d) hysteresis energy for each stress level

4. Conclusion

A characterization of a woven jute fabric reinforced polyester composite in monotonic tensile tests was firstly conducted for the two types of laminates: $[0]_8$ and $[+45/-45]_{2S}$. The AE technique and the microstructural analyzes allowed to characterize the different damage modes (matrix cracking, fibre matrix debonding and fibre breakage) and their evolution for the two layups. The cyclic fatigue behaviour was studied for the [0] samples. Tests conducted at different stress levels allowed to determine the Whöler law for the studied composite. In order to follow the damage evolution during tests, four mechanical parameters were determined (maximum and residual strain, secant modulus and hysteresis energy). The secant modulus showed that there is a stiffening effect for the low stress levels. The maximum and residual strains exhibited the same trend. Whatever the stress level, three distinct zones were observed. The same evolution as strain was observed for the hysteresis energy with a marked effect of the stress level, the higher the stress level , the more important the dissipated energy and the lower the lifetime.

Moreover, AE analyzes are in progress in order to characterize the damage modes for the fatigue tests, and to describe their evolution for the different stress levels.

References

[1] N. Godin, P. Reynaud and G. Fantozzi. *Acoustic emission and durability of composite materials*. Materials science series.New York: Wiley-ISTE editions; 2018.
[2] M. Sause, A. Gribov, A. Unwin and S. Horn. Pattern recognition appraoch to identify natural clusters of acoustic emission signals. *Pattern Recognition Letter*, 33:17-23, 2012.
[3] D. de Vasconcellos, F. Touchard and L. Chocinski-Arnault. Tension-tension fatigue behaviour of woven hemp fibre reinforced epoxy composite: A multi-instrumented damage analysis. *International journal of fatigue*, 59:159-169, 2014.
[4] S. Liang, P. Gning, L. Guillaumat. Properties evolution of flax/epoxy composites under fatigue loading. *International journal of fatigue*, 63:36-45, 2014.
[5] Y. Dobah, M. Bourchak, A. Bezazi, A. Belaadi, F. Scarpa. Multi-axial mechanical characterization of jute fibre/polyester composite materials. *Composites Part B*, 90:450-456, 2016.